Original research

Elevated glucose-6-phosphate dehydrogenase expression in the cervical cancer cases is associated with the cancerigenic event of high-risk human papillomaviruses

Tao Hu[1,2], Ya-Shan Li[1], Bo Chen[3], Ye-Fei Chang[1], Guang-Cai Liu[1], Ying Hong[1], Hong-Lan Chen[1] and Yan-Bin Xiyang[2]

[1]Department of Laboratory Medicine, The Third People's Hospital of Yunnan Province, Kunming 650011, Yunnan, China; [2]Institute of Neuroscience, Kunming Medical University, Kunming 650500, Yunnan, China; [3]Experiment Center for Medical Science Research, Kunming Medical University, Kunming 650500, Yunnan, China
The first three authors contributed equally to this work.
Corresponding author: Yan-Bin Xiyang. Email: xiyang_neuro@126.com

Abstract

The most important etiologic agent in the pathogenesis of cervical cancers (CCs) is human papillomavirus (HPV), while the mechanisms underlying are still not well known. Glucose-6-phosphate dehydrogenase (G6PD) is reported to elevate in various tumor cells. However, no available references elucidated the correlation between the levels of G6PD and HPV-infected CC until now. In the present study, we explored the possible role of G6PD in the pathology of CC induced by HPV infection. Totally 48 patients with HPV + CC and another 63 healthy women enrolled in the clinical were employed in the present study. Overall, prevalence of cervical infection with high-risk-HPV (HR-HPV) type examined was HPV-16, followed by HPV-18. The expressions of G6PD in CC samples were also detected by immunohistochemistry (IHC), qRT-PCR, and Western blot. Regression analysis showed elevated G6PD level was positively correlated with the CC development in 30–40 aged patients with HR-HPV-16/18 infection. The HPV16 + Siha, HPV18 + Hela, and HPV-C33A cell lines were employed and transfected with G6PD deficient vectors developed *in vitro*. MTT and flow cytometry were also employed to determine the survival and apoptosis of CC cells after G6PD expressional inhibition. Our data revealed that G6PD down-regulation induced poor proliferation and more apoptosis of HPV18 + Hela cells, when compared with that of HPV16 + Siha and HPV-C33A cells. These findings suggest that G6PD expressions in the HR-HPV + human CC tissues and cell lines play an important role in tumor growth and proliferation.

Keywords: Glucose-6-phosphate dehydrogenase, cervical cancer, high-risk human papillomavirus, cell proliferation, apoptosis

***Experimental Biology and Medicine* 2015; 240: 1287–1297. DOI: 10.1177/1535370214565971**

Introduction

Cervical cancer (CC) is the second most common cancer in women worldwide. Approximately 80% of primary CCs arise from pre-existing squamous dysplasia. The most important etiologic agent in the pathogenesis of CC is human papillomavirus (HPV), while the biological mechanisms have not been clearly elucidated.

It is well known that persistent high-risk HPV (HR-HPV), which has the ability to infect keratinocytes of the human skin and mucosa,[1] is a necessary and causal factor of CC.[2] HPV can be transmitted through physical contact via autoinoculation or fomites, sexual contact, as well as vertically from the HPV-positive mother to her newborn and can cause subclinical or clinical infections.[1,3] Since 1981 when a relationship was established between papillomavirus and cervical neoplasia, more than 100 different genotypes of HPV have been identified.[4] Approximately 40 HPV genotypes were found to be associated with anogenital infections and are generally classified according to their oncogenic potential into low, high, and intermediate risk types. At present, HPV16, 18, 31, 33, 35, 39, 45, 51, 52, 56, 58, and 59 were considered as HR types or oncogenic types due to their presence in high grade squamous intraepithelial lesions or CC, while HPV6, 11, 40, 42, 43, 44, 54, 61, 70, 72, and 81 are considered as low-risk (LR) types.[5] Reports reveal that HPVs are double stranded DNA viruses with an 8-kb episomal genome. The organization of the genome is divided into three functional regions: an upstream regulatory region that regulates the transcriptional and replication events; an early region

that expresses the non-structural proteins; and a late region that encodes the structural proteins L1 and L2.[6] However, the underlying pathogenesis mechanism is not well elucidated.

The pentose phosphate/hexose monophosphate shunt pathway is an alternative metabolic pathway for glucose breakdown. Upon transportation of glucose into the cell via glucose transporters, the enzyme hexokinase converts glucose to glucose-6-phosphate. Glucose-6-phosphate can then be metabolized further via glycolysis or the pentose-phosphate pathway (PPP).[7] Because of the large biosynthetic demands of a rapidly growing cancer and their need to adapt to stressful environments, the PPP has been suggested to promote cancer progression and therapy resistance.[8] Accordingly, many of the enzymes that make up the PPP are associated with malignancy,[9] including glucose-6-phosphate dehydrogenase (G6PD). G6PD, the rate-limiting enzyme of the PPP, provides ribose and NADPH that support biosynthesis and antioxidant defense. It is well known that G6PD plays an essential role in the oxidative stress response by producing NADPH. Recent available data show that G6PD elevates in various tumors, including melanoma cancer,[10] leukemia,[11] colon cancers,[12] breast cancers,[13] endometrial carcinomas,[14] etc. Considering that G6PD plays a critical role in survival, proliferation, and metastasis of cancer cells,[10] development of potent and selective G6PD inhibitors would provide novel opportunities for cancer therapy.[15,16] However, the regulation mechanism of G6PD and pathological changes in HPV-infected CC growth remains unknown.

In this study, we explored the possible pathologic role of G6PD in HPV-induced CC. Firstly, 48 CC patients infected with HPV, enrolled in the clinic of the Third People's Hospital of Yunnan Province, were served as targets. Another 63 healthy female attending physical examination were employed as normal control. The prevalence and distribution of HPV genotypes were investigated. We employed immunohistochemistry (IHC), real-time PCR, and Western blot to detect the expression of G6PD in tumor and normal adjacent tissues from the CC cases. Hematoxylin–eosin (H&E) is also used to determine the morphological changes of CC and normal adjacent tissues. The HPV16 + Siha, HPV18 + Hela, and HPV-C33A cell lines were used and transfected with G6PD deficient vectors developed *in vitro*. The expression of G6PD was then detected by real-time PCR and Western blot. 3-(4, 5-Dimethylthiazol-2-yl)-2,5-diphenyltetrazolium bromide (MTT) assay and flow cytometry were also employed to determine the survival and apoptosis of multiple CC cell lines after G6PD decrease.

Materials and methods

Ethical aspects

This study was complied with the Ethical Declaration and was approved by the Human Ethics Committee and the Research Ethics Committee of Kunming University of China. Through the surgery consent form, patients were informed that the resected specimens were kept by our hospital (Third People's Hospital of Yunnan Province) and might be used for scientific research, and that their privacy would be maintained.

Population and clinical samples collection

One hundred and twenty-four women attending the clinic in the Third People's Hospital of Yunnan Province, between February and December 2013, were invited to participate in the study. Total of 112 (90.3%) out of the 124 patients were included in this study. Patients excluded were: three (pregnancy); five (recurrent infections), two (HIV-infected), and two (other immunosuppression conditions). The excluded patients presented similar characteristics than patients included in the study.

These patients were chosen to be in the present study because they were infected with HPV as determined by our hospital. Among them, 48 histopathologically verified cervical tumor samples and matched normal adjacent tissues were obtained. These normal adjacent samples were taken at least 1 cm distal to tumor margins. The biopsies obtained were divided into two fragments immediately after surgery. One fragment was immediately stored at -80°C until nucleic acids and protein isolation. The remaining fragment was fixed in 4% formaldehyde for H&E or IHC staining.

Another 63 women registered in our hospital for health examination were also employed and served as the healthy control. They were processed for cervical cell sample collection and the subsequent HPV detection.

HPV detection and genotyping

The cervical cell sample collection for HPV detection is described as follows. Briefly, after the preparation of a Papanicolaou (Pap) smear, the brush containing cellular material was placed in a vial containing PreservCyt media (Hologic, Bedford, MA). Cell specimens in the PreservCyt media were subjected to HPV DNA genotyping by using the HPV GenoArray test kit, PCR + film chip blot (Hybribio Limited, Chaozhou, China). HPV DNA analysis was performed according to the manufactory's protocol. HPV positivity was assessed by hybridization of PCR products in an enzyme immunoassay (EIA) using two HPV oligoprobe cocktails. In addition, HPV positivity was assessed by Southern blot analysis of PCR products with a cocktail probe consisting of specific DNA fragments under low stringency conditions, allowing the detection of HPV types not included in the EIA probe cocktails. After pooling of these PCR products, typing was performed using EIA and HPV type-specific oligoprobes for the HR and LR types described above. HPV types considered HR for this analysis were 6, 11, 16, 18, 31, 33, 35, 39, 45, 51, 52, 56, 58, 59, 68, and CP8304. All other types were considered LR.

IHC and H&E staining

IHC was performed to determine the G6PD expression in normal adjacent tissue and CC tissues, as described before.[10] Briefly, tumor samples and the matched control tissues were fixed in 4% formaldehyde, embedded in paraffin wax, and then cut into 4 μm sections using a microtome. The sections were stained with H&E.

Fixed tumor samples were prepared into 30 μm frozen sections and incubated with 2% goat serum at 37°C for 20 min, followed by incubation with goat-anti-human G6PD (1:500, Santa Cruz, sc-46971) at 4°C overnight. After washing with phosphate-buffered saline (PBS), the sections were incubated with horseradish peroxidase (HRP)-conjugated rabbit anti-goat IgG (HRP-IgG) at 37°C for 30 min and colored with 3,3′-diaminobenzidine (DAB) at room temperature. PBS was substituted for the anti-G6PD antibody in negative control subjects.

Preparation of cell lines

Three human cervical carcinoma cell lines, HPV-C33A, HPV18 + Hela, and HPV16 + Siha (purchased from the Institute of Biochemistry and Cell Biology Shanghai, China), were used in this study. Cells were maintained in Dulbecco's modified Eagle medium (DMEM, Gibco, Life Technologies, Carlsbad, CA) supplemented with 10% fetal calf serum (Invitrogen, USA) at 37°C and 5% CO_2 in a humidified incubator. All cells were cultured at 70–80% of confluence.

Cell culture and gene transfection

The recombination eukaryotic plasmid (pcDNA6.2-GW/EmGFP-miR) for G6PD gene silence was employed as described before.[17] At least three silence expression sites of G6PD were designed by software supplied by Invitrogen Company. Then, we selected predesigned small interference RNA (siRNA) targeting the human G6PD gene (Gene ID, HGC:4057) and the reconstruction plasmid for G6PD knock down were designed and purchased also from Invitrogen Company (Beijing, China). The constructed recombinant plasmid was transferred into 293 T cells. Transfection efficiency was evaluated by qRT-PCR from three experiments. The target transformants with the best silencing effects were chosen and then transfected into the three kinds of CC cells. For G6PD-siRNA plasmid transfection, each cell line was prepared and incubated with the silence plasmid pcDNA6.2-GW/EmGFP-miR-G6PD (named as C33A-G6PD-silence, Hela-G6PD-silence and Siha-G6PD-silence, respectively) and non-silencing control plasmid (C33A-Empty, Hela-Empty and Siha-Empty) at 37°C, 5% CO_2 for 24 h, respectively. The transfected cells were subsequently subjected to further procedures.

Quantitative reverse-transcription PCR for G6PD

Tumor samples (60 mg) were ground under liquid nitrogen, lyzed with 1 mL of Trizol (Takara, Japan), and total RNA was extracted using Trizol (Invitrogen, USA). Total RNA (2 μg) was added to the tumor extract with Moloney Murine Leukemia Virus Reverse Transcriptase (MMLV-RT, Takara, Japan) to synthesize cDNA, and the reverse transcripts were used as the template for qRT-PCR by Tower qRT-PCR system (Analytic Jena, Germany). The qRT-PCR was conducted using 2 × Mix SYBR Green I (Biosea, USA) (10 μL), primer (0.25 μL, 10 pmol/L), template DNA (1 μL), and sterile water (8.5 μL). The PCR conditions consisted of an initial melting temperature of 95°C (3 min) followed by 39 cycles of melting (95°C, 10 s), annealing (55°C, 10 s), and extension (72°C, 30 s). A final dissociation step (95°C, 10 s; 65°C, 5 s; 95°C, 15 s) terminates the process. The real-time PCR primers used to quantify GAPDH expression were: F: 5′-CGAGATCCCTCCAAAATCAA-3′ and R: 5′-TTCAC ACCCATGACGAACAT-3′ and for G6PD were: F: 5′-A TG AGCCAGATAGGCTGGAA3-3′ and R: 5′-TAACGCAGGC GATGTTGTC-3′. All of the primers for each gene were synthesized by Invitrogen (USA). Expression of G6PD was normalized to endogenous GAPDH expression.

Western blot

Samples were lyzed on ice for 30 min in CytoBuster Protein Extraction Buffer (Novagen, USA) and centrifuged at 12,000 rpm at 4°C. The supernatant was collected and total protein concentration was measured by bicinchoninic acid (BCA) method. Fifty micrograms of protein were used for 10% sodium dodecyl sulfate-polyacrylamide gel electrophoresis (SDS-PAGE). The protein was then transferred to a nitrocellulose (NC) membrane and was sealed with Tris-buffered saline Tween-20 (TBST) containing 5% non-fat milk powder. The membrane was subsequently incubated with goat anti-human G6PD proteins (1:300, Santa Cruz, sc-46971) and mouse anti-human GAPDH (1:500, Santa Cruz, sc-81545) at 4°C overnight. After washing in TBST, the membrane was incubated with HRP-conjugated secondary antibodies (1:2000) at 25°C, and the protein quantity was determined using electrochemiluminescence (ECL) technique (BestBio, USA). The results were photographed using the JS Gel Imaging System (Peiqing, China) and the gray density was calculated using SensiAnsys software (Peiqing).

MTT assay

Cell viability was determined using the tetrazolium salt MTT assay. Briefly, cells were plated into 96-well culture plates at an optimal density of 5×10^3 cells/mL in 200 μL of culture medium per well. After 24–96 h of culture, 20 μL of 5 mg/mL MTT was added to each well and incubated at 37°C for 4 h. The medium was then gently aspirated and 150 μL of dimethyl sulfoxide (DMSO) was added to each well to solubilize the formazan crystals. The optical density of each sample was immediately measured using a microplate reader (BioRad, Hercules, CA) at 490 nm.

Flow cytometry assay

An annexin V-FITC-flow cytometry assay kit (4 A Biotech Co. Ltd.) was used to detect the apoptosis rate in the cells after G6PD-siRNA plasmid transfection, as previously described.[18] Cells were seeded into 60 mm dishes for 48 h and grown to 70–75% confluence. After quick detachment from the plate, cells were collected, washed with ice-cold PBS, and resuspended at a cell density of 1×10^6/mL in a binding buffer from the annexin V-FITC apoptosis detection kit (4 A Biotech Co. Ltd.). Cells were then stained with 5 μL of annexin V-FITC and 10 μL of propidium iodide (PI, 20 μg/mL). Cells were then incubated in the dark at 25°C for 15 min before analyzed by FACScan flow

cytometer (BD Immunocytometry Systems, San Jose, CA) and Cellquest software (BD Immunocytometry Systems) for apoptosis rate determination.

Statistical analysis

SPSS v11.5 (SPSS Inc., Chicago, IL) was used for statistical analysis. Data are presented as means ± standard deviation. Group *t* test was used to compare the expression of G6PD either between CC and normal groups or siRNA group and empty groups. Descriptive statistics and regression analyses were performed. Chi-square and Fisher's exact tests were used (when applicable) to evaluate the differences in proportions.[19] Multivariate logistic regression analysis was performed to evaluate the association between HR-HPV infection status (HPV 16/18 positive or negative), G6PD expression (IHC staining, negative/weak or positive), along with clinicopathologic characteristics of CC including age, clinical stage (FIGO stage, I–IV), cell grading (well, moderate or poor differentiation), as well as tumor diameter (≤4 or >4 cm). The strength of association was measured using odds ratios (ORs) with 95% confidence interval (CI); logistic regression was used for ordinal data to estimate adjusted ORs. The cofactors included in regression analysis were age, along with various clinicopathologic parameters, including clinical stage (FIGO stage, I–IV), cell grading (well, moderate or poor differentiation), as well as tumor diameter (≤4 or >4 cm). All hypothesis tests were set at 0.05 significance level. The statistical significance of MTT cell activity and apoptosis factions among G6PD-siRNA and empty groups was determined using one-way analysis of variance (ANOVA). The significance level was predetermined to be $P < 0.05$ unless otherwise indicated.

Results

G6PD expression in HPV + CC and normal tissues

The patients ranged in age from 31 to 78 years, with a median age of 49 years. Among the 112 cases of DNA-HPV identified by PCR, 95 (75%) were infected with HR genotypes. HPV-16 was identified in 31 (27.8%) from all HPV cases, followed by HPV-18 in 29 (25.9%), HPV-35, 52 and 58 in 6 (5.4%), HPV-11 and 62 in 4 (3.6%), HPV-6, 26, 33, 53, 82 and 89 in 3 (2.7%), HPV-51, 66, 67, 73 and 84 in 2 (1.8%), and finally HPV-11, 42, 45, 56, 59, 61, 69, 70, 72 and 92 in 1 (0.1%). The multiple-type HPV infections were 12.8%.

All 63 healthy women participated in the study provided a cervical sample for HPV analysis. They were aged 29–74 years, with a median age of 51 years. Findings for the prevalence of the various HPV types in these women were obtained. The overall prevalence of HPV infection was 16.0% (11.7–20.3%). The corresponding estimate for HR types was 60.4% (43.2–65.6%), and that for LR types was 10.9% (8.3–17.0%). HPV-16 was the most common type (18.9%). Among HR types, HPV-18, 31, 11 and 62 were each found in ≥5% of women overall. Among LR types, HPV-69 was the most common (2.5% overall), while 66, 81 and 70 were each found in 4 (0.8%) of women.

In 48 patients, which were pathologically diagnosed as CC, 93.7% (45/48) of them were found to be HPV DNA positive, and the HR-HPV16/18 rate was 85.4% (41/48). The first peak of HR-HPV infection appeared in the 30 - to 40-year-old group (52.1%), and the second peak was within the 40 - to 50-year-old group (29.1%). The multiple-type HPV infections were 16.4%, and HPV16 was the most prevalent type (32.8%), followed by HPV-18 (28.7%), HPV-29 (10.2%), HPV-35 (8.6%), HPV-52 (6.3%), HPV-58 (5.2%), and HPV-11 (5.2%). HPV-16 prevalence significantly increased with the severity to 42.8% in CC patients than that of healthy women (18.9%) without the evidence of cervical disease ($\chi^2 = 24.98$, $P < 0.05$). Age-specific prevalence of HR-HPV-16/18 estimates were the highest among 30 - to 40-year-old women and decreased with age (30–40 vs. 40–50, $\chi^2 = 17.37$, $P < 0.05$; 30–40 vs. 50–60, $\chi^2 = 23.94$, $P < 0.05$; 30–40 vs. >60, $\chi^2 = 29.61$, $P < 0.05$) (Table 1). HPV-16 prevalence was lowest among healthy women without evidence of cervical disease and significantly increased in CC patients ($\chi^2 = 19.53$, $P < 0.05$). Those patients determined with higher levels of G6PD in CC samples increased the risk of HR-HPV-18 and HPV-16 infection rate ($P < 0.05$, Table 2).

G6PD staining in normal adjacent tissue was weak relative to CC tissues that exhibited light yellow to brown staining (Figure 1). G6PD expression was significantly extensive and intensive in CC tissue (expressed in 93.75%, 45/48) than in normal adjacent tissue (expressed in 10.4%, 5/48) ($P < 0.05$).

Either qRT-PCR or Western blot analysis showed that the expression levels of G6PD in CC lesions were significantly intensive than that of normal tissues ($P < 0.05$, Figure 2). The mRNA levels of G6PD in CC were higher than that of normal tissues (1.02 ± 0.33 vs. 1.89 ± 0.21, $P = 0.000012$, <0.05, Figure 2d). A similar observation was obtained in the detection of G6PD protein expression, which showed significant elevation of G6PD protein levels in CC tissues than that of normal tissues (1.32 ± 0.23 vs. 0.53 ± 0.11, $P < 0.05$, Figure 2a–c). The association between HR-HPV status (HPV 16/18) and various clinicopathologic characteristics results determined by ORs revealed a positive trend for HR-HPV DNA detection and age (30–40, $P = 0.001$), FIGO stage III–IV (III, $P = 0.001$; IV, $P = 0.000$), cell grading (moderate, $P = 0.001$; poor, $P = 0.000$), as well as tumor diameter (>4, $P = 0.000$). Regression analysis association between G6PD expression and clinicopathologic parameters result revealed a positive trend for IHC of G6PD-positive and age (30–40, $P = 0.000$; 40–50, $P = 0.02$), FIGO stage III–IV (III, $P = 0.001$; IV, $P = 0.000$), cell differentiation (moderate, $P = 0.002$; poor, $P = 0.001$), and tumor diameter (≤4, $P = 0.001$; >4, $P = 0.000$, Table 1). G6PD levels also increased the risk of infection with HR-HPV-16/18 ($P < 0.05$, Table 2). However, HR-HPV infection (HPV-16/18 negative or positive), G6PD expression did not significantly affect the risk of developing invasive CC in women aged above 40 years (Table 1).

Stable transfection of G6PD cDNA in CC cells

The HPV-C33A, HPV18 + Hela, and HPV16+ Siha cells were stably transfected with G6PD siRNA-expressing plasmid (G6PD-silence). Control C33A, Hela, and Siha cells were transfected with empty vectors. G6PD mRNA levels

Table 1 Multivariate analysis of HPV status and G6PD expression in women diagnosed with CC ($N = 48$)[a]

	HPV status (HR-HPV-16/18)						G6PD expression (IHC detection)					
	HPV-16 -/18- Negative		HPV-16+/18+ Positive		Adjusted OR (95% CI)		G6PD negative or weak (−/±/+)		G6PD positive (++/+++/++++)		Adjusted OR (95% CI)	
	n	(%)	*n*	(%)			*n*	(%)	*n*	(%)		
Age (yr)												
30–40	2	4.2	25	52.1	**19.45**	**(11.92–28.73)**	1	2.1	28	58.3	**28.97**	**(15.18–32.67)**
40–50	3	6.3	10	29.1	1.23	(0.62–2.35)	2	4.2	11	22.9	**3.18**	**(1.21–6.06)**
50–60	1	2.1	4	8.3	1.11	(0.42–3.89)	1	2.1	2	4.2	1.31	(0.52–1.99)
>60	1	2.1	2	4.2	1.02	(0.72–1.91)	1	2.1	2	4.2	1.08	(0.49–1.84)
FIGO stage												
I	2	4.2	3	6.3	1.09	(0.59–2.12)	1	2.1	4	8.3	1.27	(0.56–1.82)
II	2	4.2	7	14.6	1.15	(0.61–2.06)	2	4.2	6	12.5	1.04	(0.42–1.76)
III	2	4.2	11	22.9	**12.69**	**(10.11–24.36)**	1	2.1	15	31.3	**19.83**	**(10.31–29.51)**
IV	1	2.1	20	41.7	**24.68**	**(16.72–31.42)**	1	2.1	18	37.5	**20.46**	**(13.25–36.24)**
Differentiation												
Well	5	10.4	5	10.4	1.32	(0.63–2.79)	2	4.2	7	14.6	1.18	(0.68–1.79)
Moderate	1	2.1	13	27.1	**8.54**	**(4.71–13.89)**	2	4.2	12	25.0	**10.83**	**(6.12–21.91)**
Poor	1	2.1	23	47.9	**32.85**	**(21.92–45.25)**	1	2.1	24	50.0	**36.35**	**(21.32–43.54)**
Tumor diameter (cm)												
≤4	6	12.5	11	22.9	2.05	(1.36–4.49)	4	8.3	15	31.3	**19.23**	**(10.03–31.47)**
>4	1	2.1	30	62.5	**45.69**	**(28.12–59.12)**	1	2.1	28	58.3	**38.62**	**(19.43–50.11)**

CI: confidence interval, OR: odds ratio.
[a]Values in bold: $P < 0.05$.

Table 2 The relationship between G6PD expression and HPV-16/18 infected in CC patients ($N = 48$)[a]

	G6PD levels (cervical cancer vs. normal adjacent tissue)			
	1.5–2.0 fold		2.0–3.0 fold	
HPV status	OR	95% CI	OR	95% CI
HPV16+	**8.65**	**3.26–13.58**	**12.98**	**5.65–19.38**
HPV18+	**21.63**	**11.32–35.69**	**38.25**	**20.16–43.82**

CI: confidence interval; OR: odds ratio.
[a]Values in bold: $P < 0.05$.

detected by qRT-PCR were significantly reduced in G6PD-silence cells compared with the matched control cells ($P < 0.05$, Figure 3).

Western blot analysis showed that the levels of G6PD protein were also significantly down-regulated in G6PD-silence cells compared with the matched control cells ($P < 0.05$, Figure 4).

Effects of G6PD on CC cells

The effect of G6PD expression on the regulation of CC cells viability was assessed. MTT assay showed that the relative proliferative capacity of G6PD-silence Hela and Siha cells grew significantly reduced at 48, 72, and 96 h compared to their control cell groups, respectively ($P < 0.05$, Figure 3). However, after G6PD-siRNA plasmid transduction, C33A cells showed no significant changes in proliferative capacity during the experimental duration (96 h), compared with that of the empty groups ($P > 0.05$, Figure 5).

Meanwhile, there was a significant increase in the apoptosis rate in G6PD-siRNA transfected cells compared to empty infected cells (Figure 6). Compared with the Siha-G6PD-silence and C33A-G6PD-silence groups, there were more apoptosis CC cells in Hela-G6PD-silence group ($P < 0.05$, Figure 6).

Discussion

The present study demonstrated that G6PD elevated in HPV-infected CC tissues and cell lines. Increased expression of G6PD was positively correlated with the cervical cancerous development in women aged 30–40 years with HR-HPV-16/18 infection. Interference of G6PD expressions by G6PD-siRNA introduction induced significant declines in proliferative capacity and increase in apoptosis of HPV16 + Siha and HPV18+ Hela cells compared with that of HPV-C33A cells. These data suggested that G6PD might be involved in the pathological changes in HR-HPV associated CC growth and development.

CC is one of the most dangerous causes of health deficiency and death worldwide. Epidemiological studies have revealed that HPV infection is an important factor contributing to CC. To some extent, the detection of HR-HPV may reduce the risk of developing CC and associated deaths.[20]

Present clinical data revealed that HR-HPV-16 and HPV-18, most prevalence genotype, significantly increased risk of developing cervical neoplasia in patients histopathologically verified as CC. This fact indicated that HPV is the

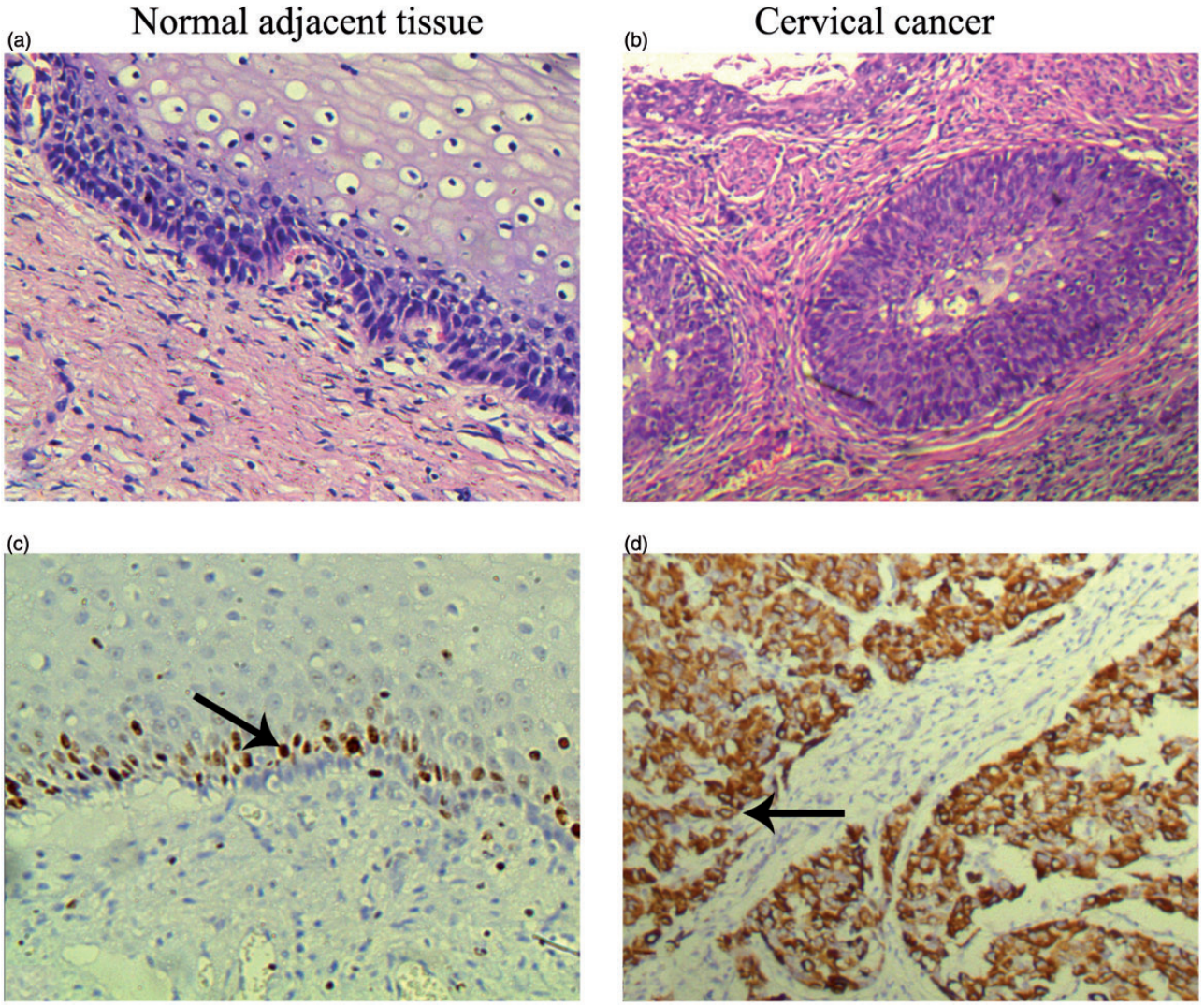

Figure 1 Morphological changes and G6PD expressions of cervical cancer and normal adjacent tissue. (a and b) Representative H&E staining files of normal adjacent (a) and cervical cancer tissues (b). (c and d) Representative IHC files of G6PD in normal adjacent (c) and cervical cancer tissues (d). There is more intense yellow or yellow-brown staining for G6PD in cervical cancer tissue than that in normal adjacent tissue. The arrows show the representative immunostaining of G6PD. Magnification: x400

principal etiological agent in cervical neoplasia.[21] Age-specific prevalence estimates were the highest among 30 - to 40-year-old women and decreased with age. Based on this fact, we assume that the age 30 and above are crucial for the development of serious cancerous lesions in Kunming region, thus this age group is the most suitable for HPV triage of laboratory medicine. It is reported that the presence of HPV has been implicated in 99.7% of the squamous cell cervical carcinoma worldwide,[22] which supported our present findings. However, the regulation mechanism of G6PD and pathological change in human CC growth associated with HPV infection remain unknown.

The present data revealed that G6PD expression significantly increased in both of CC patients and cell lines with HPV infections. It was noticed that the expression of G6PD in these cancer lesions was significantly higher than that in the adjacent normal tissue. Moreover, we also revealed that individuals, aged from 30 to 40 years, with high level of G6PD had an increased risk of developing cervical neoplasia. These findings were consistent with previous reports noting the elevated expression or activity of G6PD in tumors,[16,23–25] which suggested that intensive glucose metabolism regulated by G6PD was triggered in HPV-infected CC. We also demonstrated an effect of the combination of HR-HPV-16/18 infection and G6PD expression on the risk of development of CC in women aged 30–40. In another word, the CC patients with the HR-HPV16+/18+ and/or elevated G6PD had poor clinicopathologic characteristics.

Recent reports supported that altered glucose metabolism is one of the hallmarks of cancer, and cancer cells consume large quantities of glucose and primarily use glycolysis for ATP production, even in the presence of adequate oxygen.[26,27] While it was long suspected that this elevated glucose uptake was needed to generate ATP, it is becoming apparent that cancer cells may require sugars for

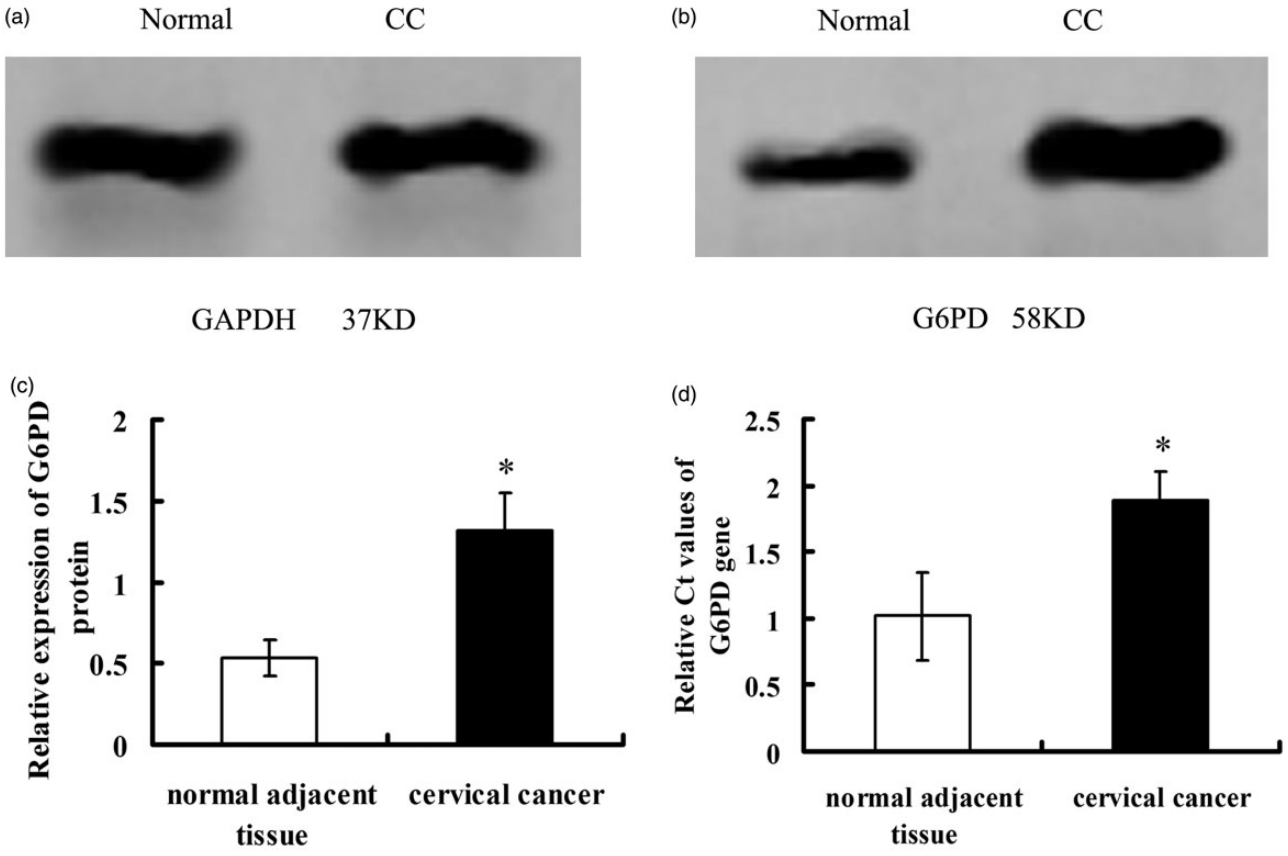

Figure 2 Expression of G6PD in cervical cancer and normal adjacent tissues. Normal, normal adjacent tissue; CC, cervical cancer tissue. (a) GAPDH detected by Western blot; (b) G6PD; (c and d) the quantitative analysis of mRNA and protein levels of G6PD. Values plotted are means ± SD ($n = 48$). *Versus human normal adjacent tissue, $P < 0.05$

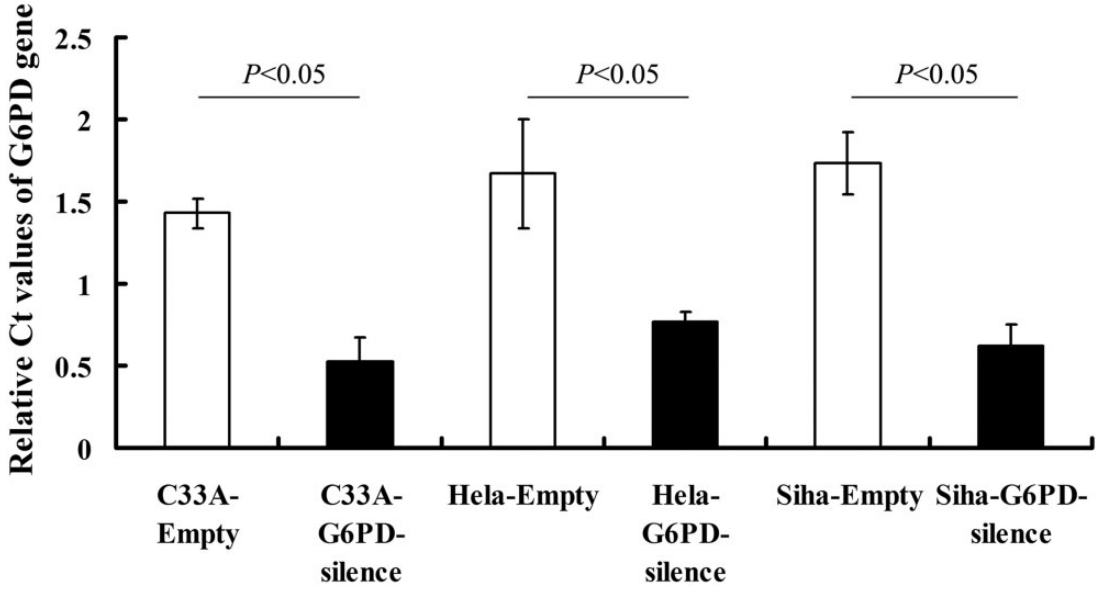

Figure 3 The mRNA levels of G6PD in various cell lines after G6PD-siRNA transfection. G6PD mRNA levels detected by qRT-PCR were significantly reduced in G6PD-siRNA transfected cells than their matched control groups ($P < 0.05$). Values plotted are means ± SD ($n = 3$). We performed each experiment at least three times and have shown a representative example

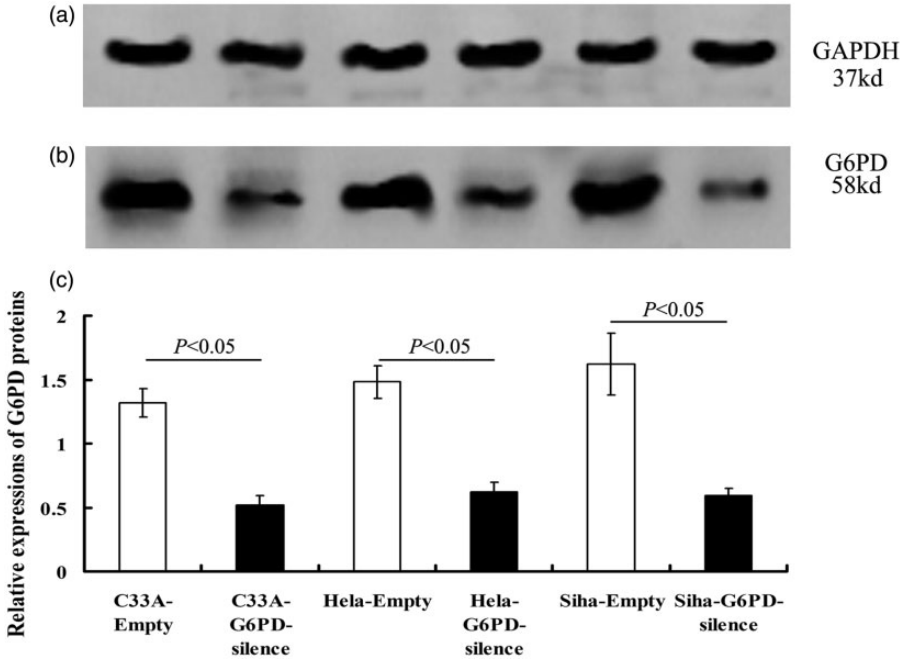

Figure 4 The protein levels of G6PD in various cell lines after G6PD-siRNA transfection. The protein levels of G6PD detected by Western blotting were significantly reduced after transfected with G6PD-siRNA ($P < 0.05$). Values plotted are means ± SD ($n = 3$)

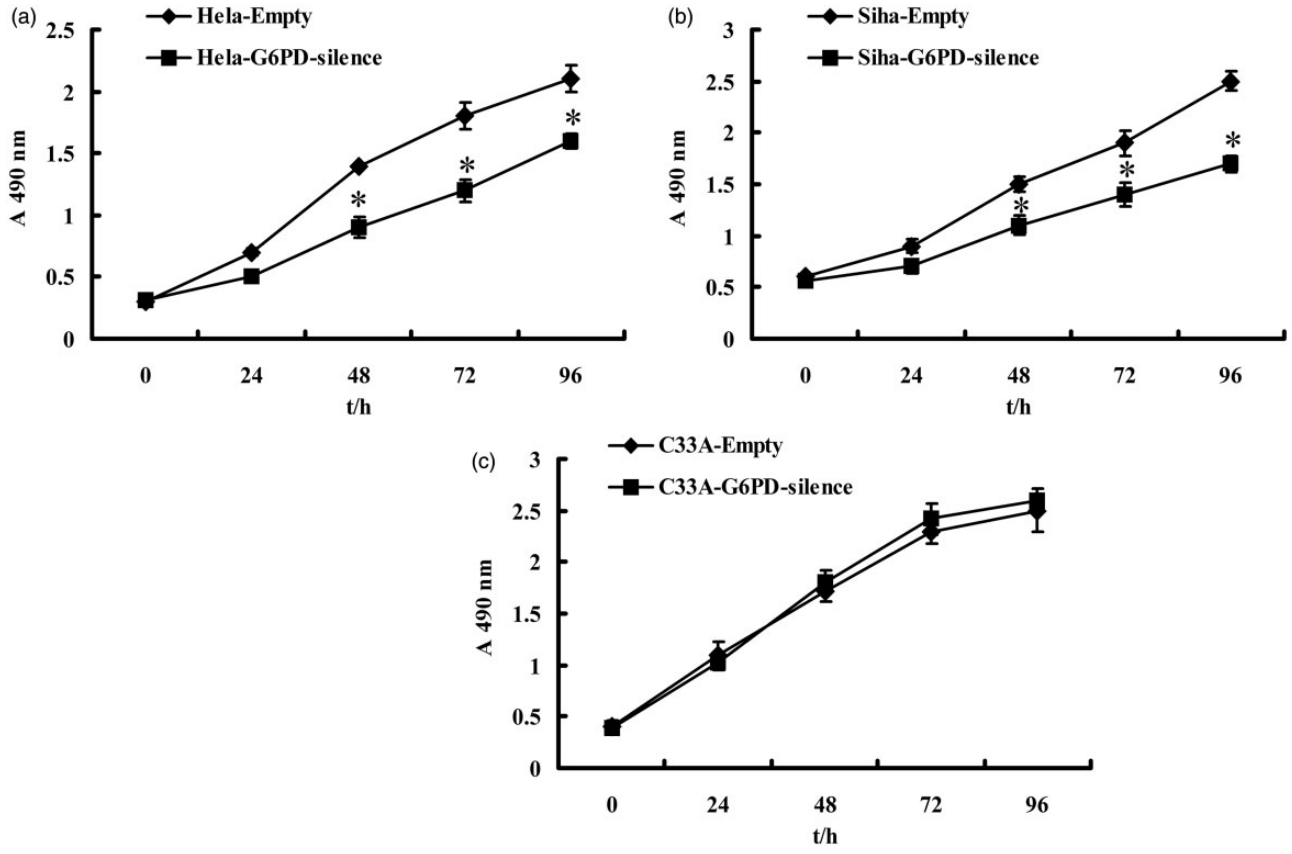

Figure 5 Effects of G6PD on cervical cancer cell proliferation. MTT assay of time-course for empty and G6PD-silence Hela, Siha, and C33A cells. After G6PD down-regulation, the cells showed a significant decrease in proliferation compared with their control ones, respectively. Values plotted are means ± SD ($n = 3$). *Versus empty cell lines, $P < 0.05$

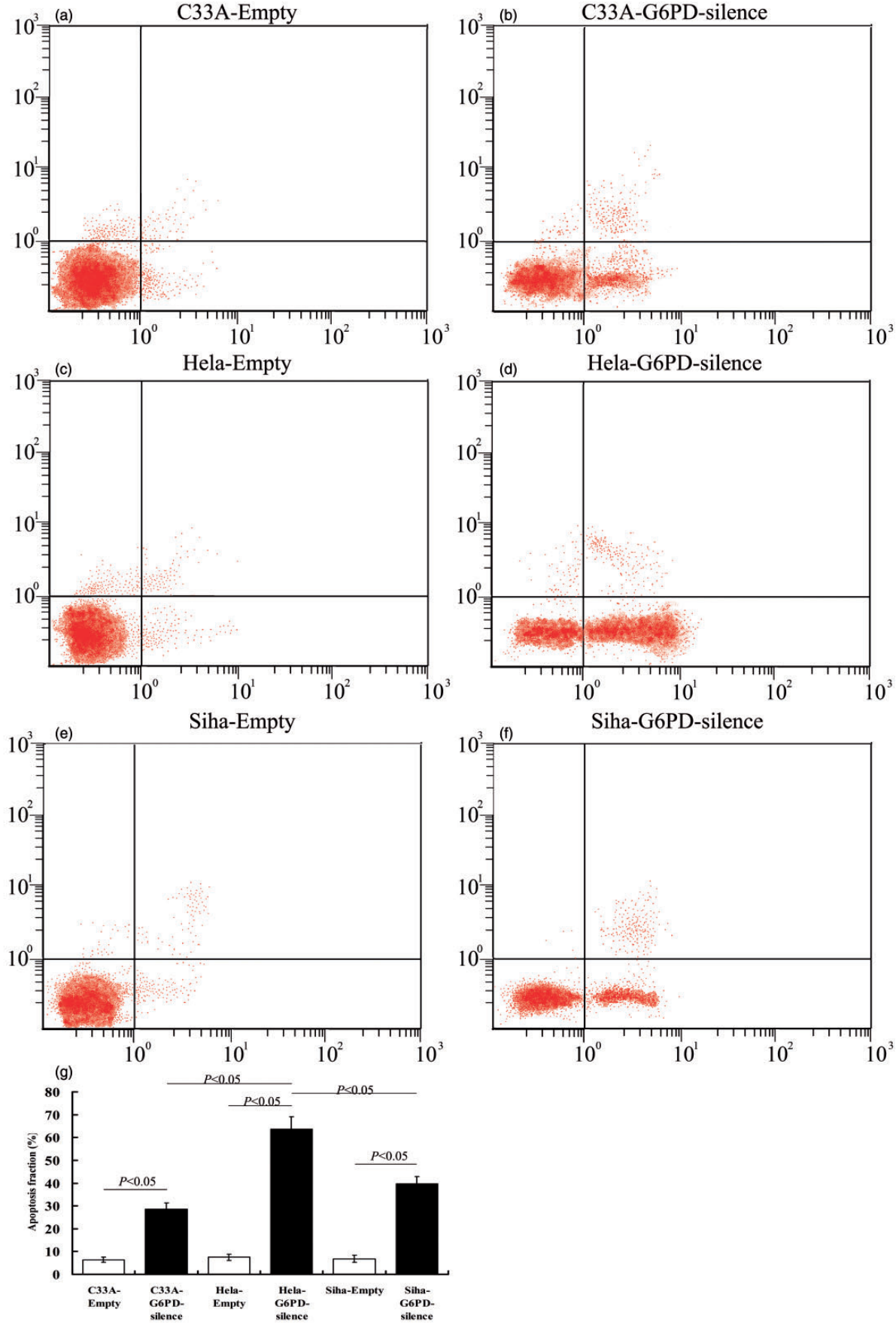

Figure 6 G6PD silence induced apoptosis in cervical cancer cells. C33A, Hela, and Siha cells were transfected with G6PD-silence or empty vector (control). (a–f) The influences of silencing G6PD on the apoptosis of C33A, Hela, and Siha cells were detected by flow cytometry. (g) Quantification shows that the percentage of apoptotic cells in G6PD-silence transfected groups is significantly higher compared with the percentage in the empty control groups. Values plotted are means ± SD ($n = 3$). *Versus empty cell lines, $P < 0.05$

many other oncogenic processes.[28,29] For example, rapidly dividing cells require a constant source of building blocks to maintain their heightened rate of biosynthetic reactions. Inherent with this increased metabolism are increased reactive oxygen species (ROS) levels, which if left unchecked, could be detrimental to the cell. As such, cancer cells also need to maintain their cellular ROS levels within a window that favors growth. Thus, oncogenic signaling pathways may promote cancer through rerouting sugar metabolism.[27] An alternative route for glucose metabolism is the PPP, which can promote both anabolic reactions and redox homeostasis. The PPP is comprised of two phases: the oxidative and non-oxidative phases. G6PD, the rate-limiting enzyme of the PPP, is responsible for the oxidation of glucose-6-phosphate to 6-phosphoglucono-d-lactone and generates NADPH as a byproduct.[7,30] Our data assessed the effect of G6PD expression on the regulation of CC cell viability. The results *in vitro* revealed that inhibition of G6PD expressions by G6PD-siRNA transfection interferes the proliferative capacity of HPV-infected human CC cell lines, Hela, and Siha. Meanwhile, there was a significant decrease in the apoptosis rate in empty-infected cells relative to G6PD-siRNA-infected HPV positive CC cells. We postulated that HPV activated the expressions of G6PD and then increased PPP flux and directed glucose to the production of NADPH and ribose, for the synthesis of macromolecules and detoxification of ROS.

Interestingly, our data also revealed that: (i) patients with HPV-18 infection had higher risk of higher G6PD levels than HPV-16 infection; (ii) HPV-18-positive Hela cells seemed to be more sensitive to G6PD decrease, when compared with that of Siha-G6PD-silence and C33A-G6PD-silence groups; (iii) HPV-negative C33A cell showed unaffected cell proliferation and lowest apoptosis rate after G6PD inhibition among the three groups. Our findings suggest that endogenous over-expression of G6PD detected in both of the human CC tissues and cell lines plays a novel role in cervical cancerous growth, proliferation, and development induced by HR-HPV-18. However, the mechanism underlying needed further investigation.

In summary, our study demonstrated that the over-expression of G6PD in CC was positively correlated with the CC development in 30- to 40-year-old patients with HR-HPV-16/18 infection. The HPV16+ Siha, HPV18+ Hela, and HPV-C33A cell lines were employed and transfected with G6PD-deficient vectors developed *in vitro*. G6PD expressional interference by siRNA introduction suppressed the proliferation and promoted apoptosis of HR-HPV-positive cells, especially HPV-18-positive Hela cells. Taken together, the present findings reveal a novel role for endogenous G6PD contributing to HPV18-dependent activated pro-survival strategies, and suggest a possible relevance of its expression levels in drug/radiotherapy resistance of HPV-18-bearing cervical carcinomas.

Author contributions: All authors participated in the design, interpretation of the studies and analysis of the data and review of the manuscript. Y-BX, TH, Y-SL, Y-FC, and G-CL were in charge of clinical samples detections and collections. BC has performed manuscript revision, finished the new data collecting and regression analysis according to the comments. Y-BX, TH, YH, and H-LC carried out cell lines cultured. Y-BX and TH wrote the manuscript.

ACKNOWLEDGMENTS

This work is supported by National Natural Science Foundation of China (Grant No. 81100911, http://isisn.nsfc.gov.cn/egrantweb/), the Special Fund of the Applied Basic Research Programs of Yunnan Province associated with Kunming Medical University in China (Grant No 2013FB116, http://61.166.241.213/). The funders had no role in study design, data collection and analysis, decision to publish, or preparation of the manuscript.

REFERENCES

1. Zur Hausen H. Papillomaviruses and cancer: from basic studies to clinical application. *Nat Rev Cancer* 2002;**2**:342–50
2. Walboomers JM, Jacobs MV, Manos MM, Bosch FX, Kummer JA, Shah KV, Snijders PJ, Peto J, Meijer CJ, Muñoz N. Human papillomavirus is a necessary cause of invasive cervical cancer worldwide. *J Pathol* 1999;**189**:12–9
3. Mammas IN, Sourvinos G, Spandidos DA. Human papilloma virus (HPV) infection in children and adolescents. *Eur J Pediatr* 2009;**168**:267–73
4. zur Hausen H, de Villiers EM, Gissmann L. Papillomavirus infections and human genital cancer. *Gynecol Oncol* 1981;**12**:S124–8
5. Muñoz N, Bosch FX, de Sanjosé S, Herrero R, Castellsagué X, Shah KV, Snijders PJ, Meijer CJ. Epidemiologic classification of human papillomavirus types associated with cervical cancer. *N Engl J Med* 2003;**348**:518–27
6. Brackmann KH, Green M, Wold WS, Rankin A, Loewenstein PM, Cartas MA, Sanders PR, Olson K, Orth G, Jablonska S, Kremsdorf D, Favre M. Introduction of cloned human papillomavirus genomes into mouse cells and expression at the RNA level. *Virology* 1983;**129**:12–24
7. Eggleston LV, Krebs HA. Regulation of the pentose phosphate cycle. *Biochem J* 1974;**138**:425–35
8. Riganti C, Gazzano E, Polimeni M, Aldieri E, Ghigo D. The pentose phosphate pathway: an antioxidant defense and a crossroad in tumor cell fate. *Free Radic Biol Med* 2012;**53**:421–36
9. Boros LG, Brandes JL, Yusuf FI, Cascante M, Williams RD, Schirmer WJ. Inhibition of the oxidative and nonoxidative pentose phosphate pathways by somatostatin: a possible mechanism of antitumor action. *Med Hypotheses* 1998;**50**:501–6
10. Hu T, Zhang C, Tang Q, Su Y, Li B, Chen L, Zhang Z, Cai T, Zhu Y. Variant G6PD levels promote tumor cell proliferation or apoptosis via the STAT3/5 pathway in the human melanoma xenograft mouse model. *BMC Cancer* 2013;**13**:251
11. Batetta B, Pulisci D, Bonatesta RR, Sanna F, Piras S, Mulas MF, Spano O, Putzolu M, Broccia G, Dessi S. G6PD activity and gene expression in leukemic cells from G6PD-deficient subjects. *Cancer Lett* 1999;**140**:53–8
12. Van Driel BE, Valet GK, Lyon H, Hansen U, Song JY, Van Noorden CJ. Prognostic estimation of survival of colorectal cancer patients with the quantitative histochemical assay of G6PDH activity and the multiparameter classification program CLASSIF1. *Cytometry* 1999;**38**:176–83
13. Polat MF, Taysi S, Gul M, Cikman O, Yilmaz I, Bakan E, Erdogan F. Oxidant/antioxidant status in blood of patients with malignant breast tumour and benign breast disease. *Cell Biochem Funct* 2002;**20**:327–31
14. Philipson KA, Elder MG, White JO. The effects of medroxyprogesterone acetate on enzyme activities in human endometrial carcinoma. *J Steroid Biochem* 1985;**23**:1059–64
15. Zhang C, Zhang Z, Zhu Y, Qin S. Glucose-6-phosphate dehydrogenase: a biomarker and potential therapeutic target for cancer. *Anticancer Agents Med Chem* 2014;**14**:280–89

16. Jiang P, Du W, Yang X. A critical role of glucose-6-phosphate dehydrogenase in TAp73-mediated cell proliferation. *Cell Cycle* 2013;**12**:3720–26
17. Xiyang YB, Lu BT, Ya-Zhao, Yuan-Zhang, Xia QJ, Zou Y, Zhang W, Quan XZ, Liu S, McDonald JW, Zhang LF, Wang TH. Expressional difference, distributions of TGF-β1 in TGF-β1 knock down transgenic mouse, and its possible roles in injured spinal cord. *Exp Biol Med (Maywood)* 2014;**239**:320–29
18. Rasola A, Geuna M. A flow cytometry assay simultaneously detects independent apoptotic parameters. *Cytometry* 2001;**45**:151–7
19. Jemal A, Bray F, Center MM, Ferlay J, Ward E, Forman D. Global cancer statistics. *CA A Cancer J Clin* 2011;**61**:69–90
20. Levin CE, Sellors J, Shi JF, Ma L, Qiao YL, Ortendahl J, O'Shea MK, Goldie SJ. Cost-effectiveness analysis of cervical cancer prevention based on a rapid human papillomavirus screening test in a high-risk region of China. *Int J Cancer* 2010;**127**:1404–11
21. Boldrini NT, Freitas LB, Coutinho AR, Loureiro FZ, Spano LC, Miranda AE. High-grade cervical lesions among women attending a reference clinic in Brazil: associated factors and comparison among screening methods. *PLoS One* 2014;**9**:e102169
22. Walboomers JM, Jacobs MV, Manos MM, Bosch FX, Kummer JA, Shah KV, Snijders PJ, Peto J, Meijer CJ, Muñoz N. Human papillomavirus is a necessary cause of invasive cervical cancer worldwide. *J Pathol* 1999;**189**:12–9
23. Frederiks WM, Bosch KS, Hoeben KA, van Marle J, Langbein S. Renal cell carcinoma and oxidative stress: the lack of peroxisomes. *Acta Histochem* 2010;**112**:364–71
24. Ramão A1, Gimenez M, Laure HJ, Izumi C, Vida RC, Oba-Shinjo S, Marie SK, Rosa JC. Changes in the expression of proteins associated with aerobic glycolysis and cell migration are involved in tumorigenic ability of two glioma cell lines. *Proteome Sci* 2012;**10**:53
25. Wang J, Yuan W, Chen Z, Wu S, Chen J, Ge J. Overexpression of G6PD is associated with poor clinical outcome in gastric cancer. *Tumour Biol* 2012;**33**:95–101
26. Hanahan D, Weinberg RA. Hallmarks of cancer: the next generation. *Cell* 2011;**144**:646–74
27. Tsouko E, Khan AS, White MA, Han JJ, Shi Y, Merchant FA, Sharpe MA, Xin L, Frigo DE. Regulation of the pentose phosphate pathway by an androgen receptor-mTOR-mediated mechanism and its role in prostate cancer cell growth. *Oncogenesis* 2014;**3**:e103
28. Ward PS, Thompson CB. Metabolic reprogramming: a cancer hallmark even Warburg did not anticipate. *Cancer Cell* 2012;**21**:297–308
29. Wittig R, Coy JF. The role of glucose metabolism and glucose-associated signaling in cancer. *Perspect Med Chem* 2008;**1**:64–82
30. Kruger NJ, von Schaewen A. The oxidative pentose phosphate pathway: structure and organisation. *Curr Opin Plant Biol* 2003;**6**:236–46

(Received August 17, 2014, Accepted November 10, 2014)